



| | |
|-------------------------------------|--|
| Title | Simplified Elastic Model for Restraining Effects of Backfill Soil on Integral bridges |
| Authors(s) | Lehane, Barry M., Keogh, D.L., O'Brien, Eugene J. |
| Publication date | 1999-10 |
| Publication information | Lehane, Barry M., D.L. Keogh, and Eugene J. O'Brien. "Simplified Elastic Model for Restraining Effects of Backfill Soil on Integral Bridges." Elsevier, October 1999. https://doi.org/10.1016/S0045-7949(98)00247-8 . |
| Publisher | Elsevier |
| Item record/more information | http://hdl.handle.net/10197/4048 |
| Publisher's statement | This is the author's version of a work that was accepted for publication in Computers and Structures. Changes resulting from the publishing process, such as peer review, editing, corrections, structural formatting, and other quality control mechanisms may not be reflected in this document. Changes may have been made to this work since it was submitted for publication. A definitive version was subsequently published in Computers and Structures (VOL73, ISSUE1-5, (1999)) DOI:10.1016/S0045-7949(98)00247-8 Elsevier Ltd. |
| Publisher's version (DOI) | 10.1016/S0045-7949(98)00247-8 |

Downloaded 2025-12-04 22:46:38

The UCD community has made this article openly available. Please share how this access benefits you. Your story matters! (@ucd_oa)



© Some rights reserved. For more information

Simplified Model for Restraining Effects of Backfill Soil on Integral Bridges

B.M. Lehane, D.L. Keogh and E.J. O'Brien

**Department of Civil, Structural & Environmental Engineering, Trinity College,
Dublin 2, Ireland**

Abstract

This paper presents the formulation of a simple method for the prediction of the additional stresses induced in frame type integral bridges due to thermal expansion of the deck. These stresses are controlled to a large extent by the restraint provided to the deck by the backfill soil adjacent to the abutments. The first part of the paper develops a realistic means of assessing appropriate stiffness values for the backfill; the approach presented makes use of results from recent high quality laboratory soil testing. A boundary element type approach is then used to derive approximate general expressions, written in terms of the soil stiffness and the flexural rigidity of the abutment, for the lateral and rotational restraint provided by both the abutment and soil. These expressions are subsequently manipulated into a form that enables designers to make use of standard frame analysis computer programs for the prediction of thermal expansion effects. The proposed method is shown to compare well with predictions obtained using a finite element model of the soil and structure.

1 Background

An integral bridge is one in which the bridge deck and its supporting abutments and piers are integrated to form a continuous framed structure. Although many existing traditional masonry and reinforced concrete arch bridges are of integral form, designers have, in recent times, favoured the isolation of the deck from its supports by means of bearings and expansion joints. The introduction of these features has resulted in an increased susceptibility to attack from the ingress of water and de-icing salts which have, in many cases, led to excessive maintenance and rehabilitation costs. Such instances have brought about renewed interest in maintenance free integral bridge construction.

Integral bridges have been used successfully in many countries, particularly in the USA and Canada, where overall deck lengths of up to 240m have been constructed. In the UK, it has been proposed [1] that all bridges with lengths of up to 60m and a skew of less than 30° be constructed integrally. Although many of the integral bridges in current use perform satisfactorily in service, there is some uncertainty amongst designers as to the degree of restraint provided by the surrounding soil to the bridge. An accurate assessment of this restraint is essential for the estimation of the additional forces

and moments induced in the deck caused by its longitudinal expansion; such expansion takes place in response to temperature increases during both daily and seasonal temperature variations and leads to increases in axial stress and hogging moment in the deck.

This paper is concerned with the effects of deck thermal expansion on frame type integral bridges of the type shown in Figure 1. The effects of longitudinal deck movements in integral bridges supported on shallow foundations (or bank seats), where the lateral resistance is dominated by the sliding capacity of the footing, is the subject of another project currently underway at Trinity College Dublin. The consequences of deck contraction and expansion in instances where the base is pinned and the soil resistance may be ignored have been discussed by O'Brien and Flanagan [2].

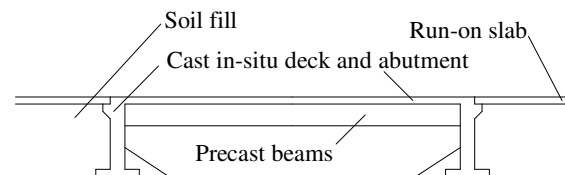


Figure 1: Frame Integral Bridge

2 Outline of Approach

An assessment of forces induced by thermal expansion in integral bridges (of the type shown in Figure 1) would commonly be made using a standard frame analysis computer package in which the soil is modelled as a series of linear springs. Such an approach, although relatively straightforward, is unrealistic as this representation of soil does not allow for the fact that movement at one level within the soil causes changes in stress at other levels. In addition, there is no satisfactory theory from which the spring constant (or modulus of subgrade reaction) can be derived.

Given these limitations, a simple predictive method (i.e., one which does not require use of the finite element method and a complex constitutive relationship for the soil) was

pursued which would model the backfill soil as a continuum with properties that were realistic and easily assessed.

The steps followed in the development of the predictive method described in this paper were:

- (i) formulation of an expression for the stiffness of the backfill using results from recent research on the stiffness properties of cohesionless soils; this expression allows the designer to assess an appropriate equivalent linear stiffness modulus for the soil.
- (ii) derivation of an approximate matrix, in terms of a linear stiffness modulus for the soil and the flexural rigidity of the abutment, that represents the lateral and rotational stiffness offered to the bridge deck by the abutment and soil.
- (iii) use of the matrix derived in (ii) to develop a simple predictive model which allows thermal expansion effects to be estimated using a standard frame analysis computer program.

The proposed approach is validated by comparison with a finite element model of the bridge and soil.

3 Stiffness of Backfill Material

Backfill employed behind abutments is conventionally a free draining cohesionless material which is often compacted to minimise the length of the run-on slab. The degree of restraint provided to the bridge deck as it attempts to expand depends primarily on the stiffness characteristics of this backfill as well as on the flexural rigidity of the abutment. Appropriate modelling of this backfill is therefore vital to the accuracy of the analytical predictions.

3.1 General trends shown by cohesionless soils

The stiffness properties of siliceous cohesionless materials have been summarised in detail by many workers [3, 4, 5]. Four of the most significant of the findings relevant to abutment backfill are:

- (i) Stiffness increases as the density increases or the void ratio (e) reduces. Tatsouka & Shibuya [3] and others, have confirmed that a suitable normalising function for the shear stiffness of clean siliceous granular deposits is given by:

$$F(e) = (2.17 - e)^2 / (1 + e) \quad (1)$$

The dry density (ρ_d) of the backfill is related to the void ratio (e) by the expression:

$$\rho_d = G_s / (1 + e) \quad (2)$$

where G_s is the specific gravity of the soil particles (≈ 2.65).

- (ii) Stiffness is approximately proportional to the square root of the current mean effective stress (p') at very small strains but varies in direct proportion to p' at strains in excess of about 0.1%. (p' is defined as the mean of the effective stresses acting in the three principal stress directions.)

- (iii) At a given density and stress level, the stiffness of a granular deposit reduces by a factor of between two and four for each log cycle increase in strain above the linear elastic limit (which is generally between 0.001% and 0.01%). Figure 2 shows typical examples of the variation

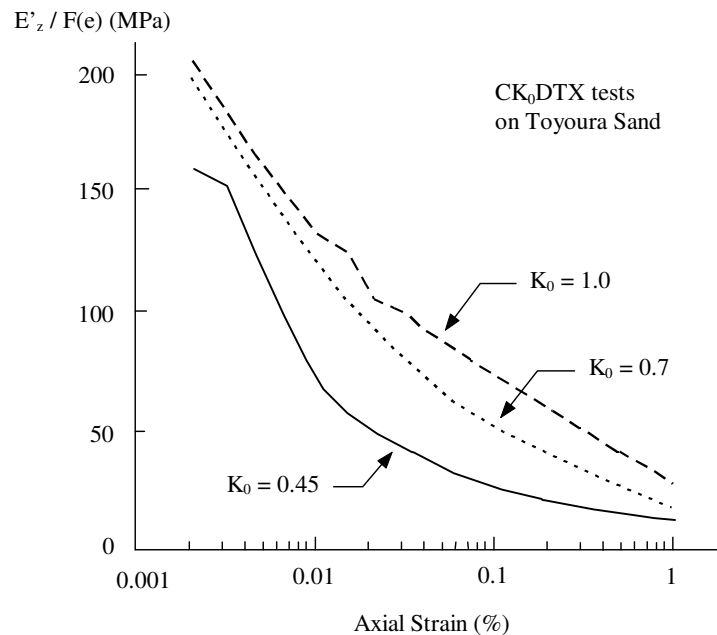


Figure 2: Typical Examples of the Variation of Stiffness (expressed as the secant Young's modulus) with Strain

of stiffness (expressed as the vertical secant Young's modulus, E'_z) with vertical strain; these were measured in

triaxial tests on sand samples with different consolidation histories.

(iv) Other factors affecting stiffness include: the previous direction of loading, the degree of ageing, the angularity of the deposit, the anisotropy and the shearing mode to which it is subjected to (see, for example, [5]).

3.2 Database of Soil Stiffness Measurements

The applicability of these general trends is examined in the following for a range of laboratory small strain stiffness measurements made on reconstituted siliceous sands and

gravels. This review focused on recent tests for which the variation of shear stiffness (G) with shear strain (γ) was presented over the strain ranges of interest and where sufficient details concerning the tests and samples were reported. The data base assembled, which is listed in Table 1, comprises 6 K_0 consolidated and 10 isotropically consolidated drained triaxial tests (CK₀DTX and CIDTX), 5 K_0 consolidated undrained triaxial tests (CK₀UTX) and 8 undrained torsional simple shear (TSS) tests. In all, 29 tests on a total of nine cohesionless deposits are examined.

| No. | Material | Test Type | D ₅₀ (mm) | e | σ' _{v0} (kPa) | σ' _{h0} (kPa) | OCR | G _{0.01} (MPa) | G _{0.1} (MPa) |
|---|--------------------------------|---------------------|-------------------------|------|---------------------------|---------------------------|-----|----------------------------|---------------------------|
| 1 | Labenne sand [6] | CK ₀ UTX | 0.3 | 0.62 | 103 | 57 | 1 | 32 | 8 |
| 2 | | CK ₀ UTX | 0.3 | 0.62 | 70 | 48 | 1.4 | 91 | 19 |
| 3 | | CK ₀ UTX | 0.3 | 0.62 | 15 | 21 | 7 | 27 | 13 |
| 4 | Thames Gravel [7] | CK ₀ DTX | 2.0 | 0.46 | 102 | 61 | 1.4 | 110 | 28 |
| 5 | | CK ₀ DTX | 2.0 | 0.46 | 188 | 112 | 1.4 | 175 | 31 |
| 6 | | CK ₀ UTX | 2.0 | 0.59 | 102 | 61 | 1.4 | 105 | 23 |
| 7 | | CK ₀ UTX | 2.0 | 0.42 | 102 | 61 | 1.4 | 135 | 30 |
| 8. | Thanet Sand [8] | CIDTX | 0.1 | 0.76 | 300 | 300 | 1.1 | 100 | 63 |
| 9. | | CIDTX | 0.1 | 0.76 | 500 | 500 | 1.1 | 129 | 75 |
| 10. | | CIDTX | 0.1 | 0.74 | 600 | 600 | 1.1 | 290 | 94 |
| 11. | | CIDTX | 0.1 | 0.74 | 800 | 800 | 1.1 | 253 | 113 |
| 12. | | CIDTX | 0.1 | 0.74 | 1000 | 1000 | 1.1 | 292 | 135 |
| 13. | Toyoura Sand (reported in [5]) | CK ₀ DTX | 0.15 | 0.79 | 100 | 45 | 1 | 32 | 12 |
| 14. | | CK ₀ DTX | 0.15 | 0.79 | 100 | 70 | 1 | 52 | 22 |
| 15. | | CK ₀ DTX | 0.15 | 0.79 | 100 | 100 | 1 | 56 | 31 |
| 16. | | CK ₀ DTX | 0.15 | 0.79 | 100 | 150 | 1 | 63 | 42 |
| 17. | Toyoura Sand [9] | CIDTX | 0.15 | 0.67 | 78 | 78 | 1 | 76 | 43 |
| 18. | Leighton Buzzard [9] | CIDTX | 0.60 | 0.55 | 15 | 15 | 1 | 48 | 14 |
| 19. | Ticino Sand [9] | CIDTX | 0.55 | 0.66 | 49 | 49 | 1 | 54 | 27 |
| 20. | Hime Gravel [10] | CIDTX | 1.9 | 0.55 | 49 | 49 | 1 | 107 | 48 |
| 21. | Crushed sandstone [11] | CIDTX | - | 0.22 | 78 | 78 | 1 | 150 | 108 |
| 22. | Ham River Sand [12] | TSS | 0.4 | 0.77 | 299 | 263 | 3 | 112 | 65 |
| 23. | | TSS | 0.4 | 0.77 | 109 | 95 | 3 | 55 | 23 |
| 24. | | TSS | 0.4 | 0.77 | 606 | 297 | 1 | 119 | 70 |
| 25. | | TSS | 0.4 | 0.77 | 300 | 147 | 1 | 72 | 35 |
| 26. | Toyoura Sand (reported in [3]) | TSS | 0.15 | 0.69 | 196 | 66 | 1 | 69 | 30 |
| 27. | | TSS | 0.15 | 0.69 | 98 | 57 | 2 | 80 | 37 |
| 28. | | TSS | 0.15 | 0.69 | 98 | 39 | 1 | 53 | 18 |
| 29. | | TSS | 0.15 | 0.69 | 49 | 49 | 4 | 62 | 24 |
| Note: D ₅₀ = mean particle size, σ' _{v0} and σ' _{h0} are initial vertical and horizontal effective stresses acting on samples, OCR = overconsolidation ratio, G _{0.01} and G _{0.1} = shear stiffnesses at shear strains of 0.01% and 0.1% respectively | | | | | | | | | |

Table 1: Database of Laboratory Stiffness Measurements

The shear stiffness of the samples measured at shear strains of 0.01% and 0.1% (G_{0.01} & G_{0.1}) divided by the void ratio function, F(e), are plotted in Figure 3 against the mean effective

stress (p') divided by atmospheric pressure (p_{atm}). Plotted in this form, it is evident that stiffness at a given strain, normalised to take account of density variations, is strongly dependent on the

mean effective stress level (p'). The scatter about the mean trend lines on this figure can be explained by the other, previously mentioned, factors known to affect stiffness.

Further examination of the test results of the samples in the data base indicated that the variations of shear stiffness with strain above the linear elastic limit could be approximated as a power function of the strain level, i.e.:

$$G = f(\gamma^n) \quad (3)$$

This is illustrated in Figure 4 which re-plots the Young's moduli (E_z') of Figure 2 using logarithmic axes. It is evident that lines of slope ' n ', varying between 0.3 and 0.45, closely match the experimental curves. The mean n value derived for all samples in the database was 0.4.

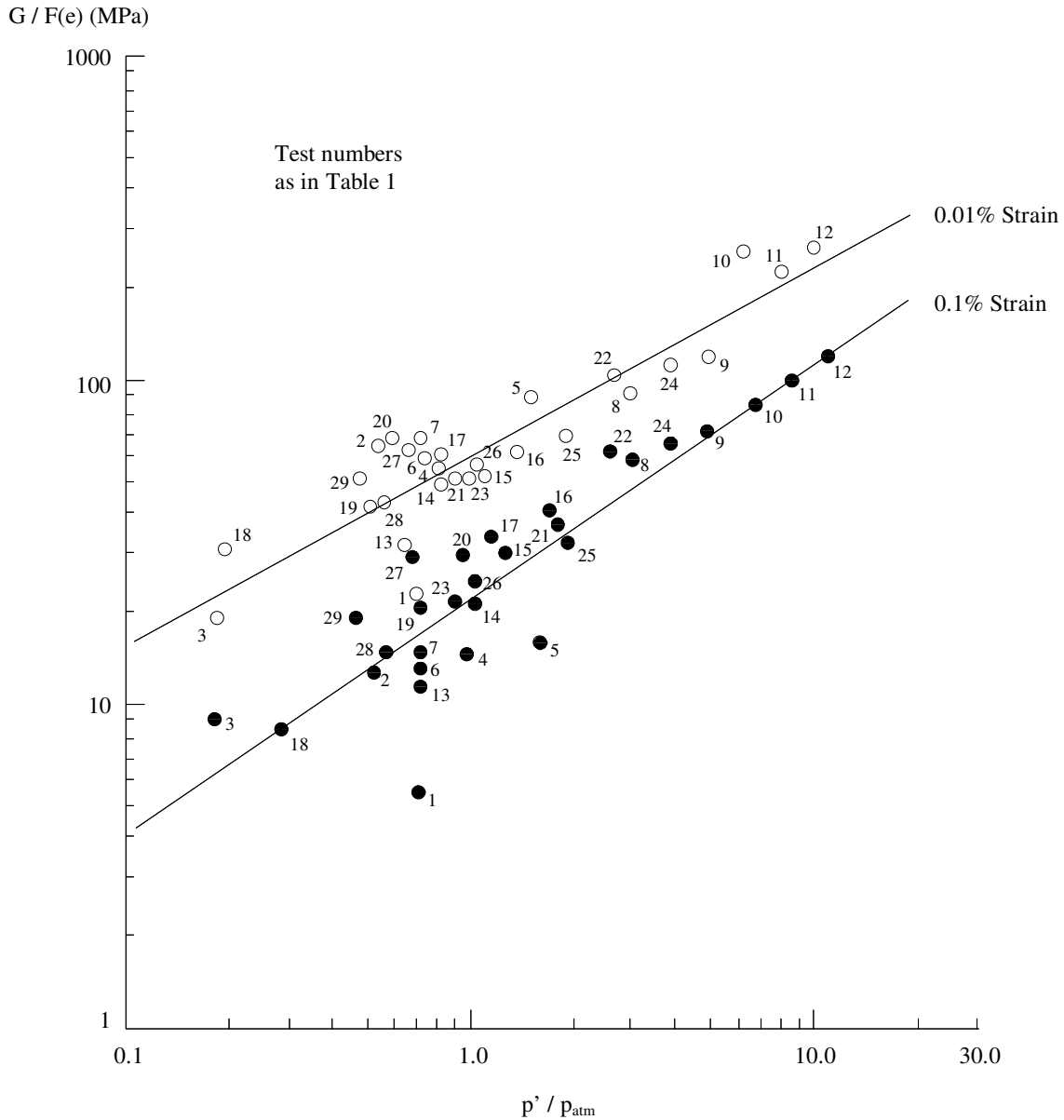


Figure 3: Shear Stiffness Divided by Void Ratio Function versus Mean Effective Stress Divided by Atmospheric Pressure

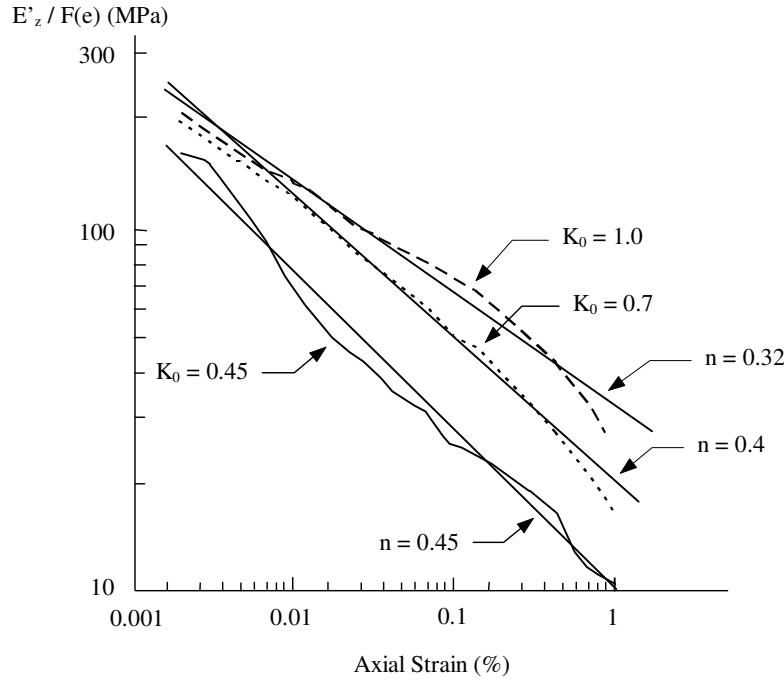


Figure 4: Young's Moduli of Figure 2 re-plotted using Logarithmic Axes

3.3 Soil Stiffness Correlation for Cohesionless Soils

The foregoing review has highlighted the need to model the dependence of the stiffness of cohesionless soils on density (or void ratio), stress level and strain level when describing the behaviour of the backfill adjacent to abutments. To avoid unnecessary complications in the derivation of an appropriate expression for the backfill stiffness, it was assumed when analysing the database listed in Table 1 that the degree of non-linearity of stiffness with strain is approximately constant for all soils (i.e. n is constant) and that stiffness is proportional to the square root of the mean effective stress at all strain levels. Shear moduli (G) were converted to equivalent Young's moduli (E_s) taking $\nu' = 0.25$ and $E_s = 2G(1 + \nu')$ and the following best fit correlation was obtained:

$$E_s \text{ (MPa)} \approx 2.5G \text{ (MPa)} = 150F(e) \left(\frac{p'}{p_{atm}} \right)^{0.5} \left(\frac{0.01}{\gamma} \right)^{0.4} \quad (4)$$

with γ expressed as a percentage and $0.005\% < \gamma < 1\%$. This expression is in good general agreement with trends reported at the recent 'pre-failure deformation of geomaterials' conference in Sapporo, Japan (see, for example, [13]).

3.4 Equivalent Elastic Stiffness for the Abutment Soil

Figure 5 presents values of the Young's moduli (E_s) for the backfill soil, derived using Equation 4, for a range of in-situ dry densities (ρ_d), mean effective stresses (p') and average shear strain levels (γ). The designer should be aware of the following details when selecting an appropriate E_s value from this plot.

(i) The additional axial forces and hogging bending moments induced in integral bridge decks due to thermal expansion of the deck become larger as the degree of restraint and hence stiffness of the backfill soil increases. The design stiffness should therefore be a maximum credible value. In addition, it may be conservatively assumed that the backfill does not reach the passive limiting condition.

(ii) Cyclic variations in temperature (and associated expansions and contractions of the deck) will cause the backfill to compact and, with time, to tend to an equilibrium density compatible with the strain amplitude that it is regularly subjected to. It might be assumed that the granular backfill at this stage will have increased in density by up to 10% from its as-placed density.

(iii) Centrifuge tests reported by Springman & Norrish [14] have shown that the pressure distribution acting on an abutment following cyclic expansions and contractions of the deck is similar in form to the classical compaction stress distribution proposed by Ingold [15] in which horizontal stresses remain approximately constant to depths of up to 6m and typically have magnitudes of between 25 kPa and 50 kPa (depending on the type of compaction plant used). This observation suggests that use of a *constant* soil stiffness value with depth (for a given strain) is reasonably realistic and that upperbound mean effective stresses (p') in operation during deck expansion lie between about 50kPa and 100kPa.

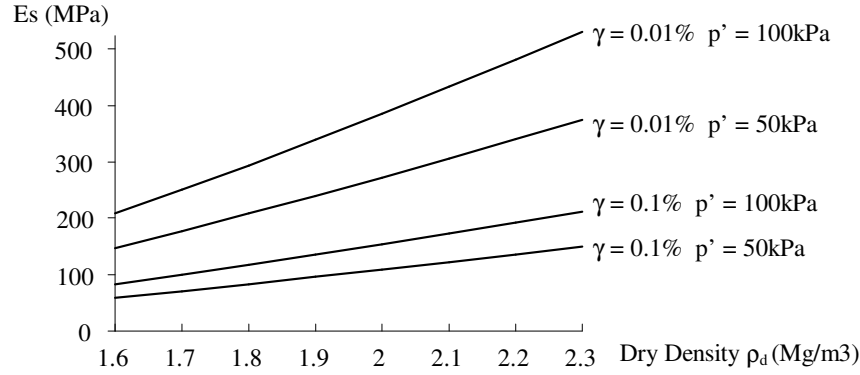


Figure 5: Young's Modulus (E_s) of Backfill Soil for a range of In-Situ Dry Densities (ρ_d), Mean Effective Stresses (p') and Average Shear Strain Levels (γ)

(iv) Strain levels induced by thermal expansion of the deck vary within the backfill and reduce with increasing distance from the deck-abutment connection where they are at a maximum. In selecting an appropriate equivalent linear elastic stiffness for the backfill, the designer must therefore ensure that its value is compatible with the average strain level in the vicinity of the abutment. Data presented by Card & Carder [16] and Springman & Norrish [14] and results from a number of finite element predictions of the type described later in this paper suggest that a suitable lower bound average shear strain is likely to be in the range $\delta/10$ to $\delta/20$ (where δ is half the thermal expansion of the deck, expressed in metres).

Although the adoption of a linear elastic modulus for the backfill is clearly incompatible with Equation 4 and points (ii), (iii) and (iv) above, it will be seen later that predictions of the additional stresses induced in the deck due to its thermal expansion are not particularly sensitive to the precise value of soil stiffness. Use of an appropriate linear modulus (estimated from Figure 5) will therefore be sufficient for most design situations.

4 Soil-Structure Interaction Analysis

A stiffness matrix, derived using the OASYS finite element computer code SAFE [17], was used to model the soil as an elastic continuum of uniform stiffness (E_s). The inverse of this matrix (i.e. the flexibility matrix) defines the magnitude of the displacements at 40 equally spaced nodes on the vertical free surface AB, shown in Figure 6, due to a unit load applied at any one of the nodes. The OASYS retaining wall program FREW [17, 18] combines this soil stiffness matrix with a matrix derived for the wall; this wall is represented by elastic beam elements in between nodes on the vertical boundary AB and may have a length shorter than the depth of the soil block (H). The program allows rotational and horizontal restraints to be applied at any node.

The stiffness matrix representing the horizontal and rotational restraint provided by the abutment and soil was derived by performing a parametric study using the FREW program. This study examined abutments of varying flexural rigidities (EI_a) and depths (D) and soil blocks of varying stiffness (E_s) and height (H). An implicit assumption in the

analysis was that of zero load transfer from the base of the abutment to the soil.

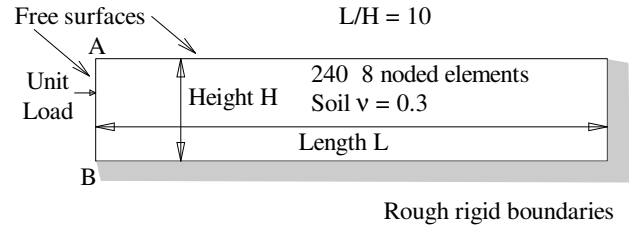


Figure 6: Elastic Soil Block used for Finite Element Computations

The analyses involved applying (i) a horizontal displacement δ with zero rotation and (ii) a unit rotation θ with zero displacement to the top of the abutment for each set of input parameters. It was found that the flexural rigidity of the abutment EI_a and the ratio r , defined as the soil stiffness E_s divided by EI_a , were the most important factors controlling the computed magnitudes of the lateral forces F_h and moments M induced at the top of the abutment.

In contrast to the 'no soil' condition (as examined by O'Brien & Flanagan [2]), the depth of the abutment (D) had little influence on F_h and M for retained heights in excess of 5m. Further analyses indicated that F_h and M showed only slight reductions as the height of the soil block (H) was increased above 5m. Such findings are in keeping with the 'long pile' concept commonly introduced in the analysis of laterally loaded piles.

The results of computations carried out for EI_a values in the range 1×10^4 to 5×10^6 kNm² and E_s values in the range 10 MPa to 500 MPa are presented in Figure 7; results are plotted as ratios of computed values of $M/(EI_a\delta)$, $F_h/(EI_a\delta)$, $M/(EI_a\theta)$ and $F_h/(EI_a\theta)$ against ' r ' using logarithmic axes. Points plotted represent the mean computed value of each ratio for each value of r examined. Both the depth of the abutment (D) and the height of the soil block (H) were taken as 10m for these analyses so that typical values (if not slight overestimates) of the lateral and rotational stiffnesses provided by abutments embedded in backfill could be derived.

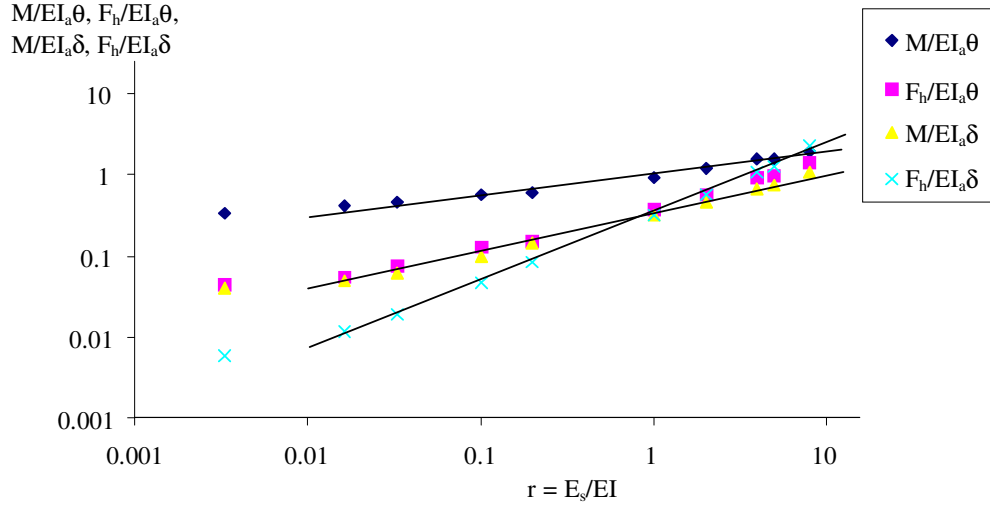


Figure 7: Ratios of $M/(EI_a \delta)$, $F_h/(EI_a \delta)$, $M/(EI_a \theta)$ and $F_h/(EI_a \theta)$ Varying with r

The ratios $M/(EI_a \delta)$, $F_h/(EI_a \delta)$, $M/(EI_a \theta)$ and $F_h/(EI_a \theta)$ are seen in Figure 7 to vary linearly with r (for $r > 0.01 \text{ m}^{-4}$) when logarithmic axes are used; each ratio may therefore be described as a power function of r . It can also be seen that, in keeping with elastic theory, the computations showed the ‘cross-terms’ $F_h/(EI_a \theta)$ and $M/(EI_a \delta)$ to be essentially equal for any given value of r .

The predictions may be summarised by the following expression which describes the *best fit* lines to the results shown in Figure 7; the 2×2 matrix represents the lateral and rotational resistance of the abutment to a lateral displacement (δ) and rotation (θ):

$$EI_a \begin{bmatrix} r^{0.75} / 3.5 & -r^{0.5} / 3 \\ -r^{0.5} / 3 & r^{0.25} \end{bmatrix} \begin{Bmatrix} \delta \\ \theta \end{Bmatrix} = \begin{Bmatrix} F_h \\ M \end{Bmatrix} \quad (5)$$

When a frame bridge with an abutment height of H is pinned at the supports and the system of fixities illustrated in Figure 8 is used,

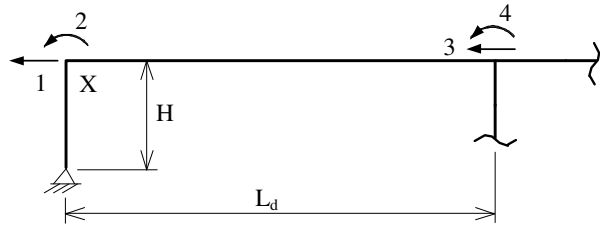


Figure 8: Portion of Frame Bridge with Pinned Supports

the stiffness matrix, $[K]$, in the absence of soil, is:

$$[K] = \begin{bmatrix} \frac{EA_d}{L_d} + \frac{3EI_a}{H^3} & -\frac{3EI_a}{H^2} & \dots & \dots \\ -\frac{3EI_a}{H^2} & \frac{4EI_d}{L_d} + \frac{3EI_a}{H} & \dots & \dots \\ \vdots & \vdots & \ddots & \vdots \\ \vdots & \vdots & \dots & \dots \end{bmatrix} \quad (6)$$

where A_d , L_d and I_d are the cross-sectional area, length and second moment of area of the deck span respectively. When the bridge is embedded in soil and this is taken into account, the terms involving I_a are replaced with terms from Equation 5 and Equation 6 then becomes:

$$[K_c] = \begin{bmatrix} \frac{EA_d}{L_d} + \frac{EI_a r^{0.75}}{3.5} & -\frac{EI_a r^{0.5}}{3} & \dots & \dots \\ -\frac{EI_a r^{0.5}}{3} & \frac{4EI_d}{L_d} + EI_a r^{0.25} & \dots & \dots \\ \vdots & \vdots & \ddots & \vdots \\ \vdots & \vdots & \dots & \dots \end{bmatrix} \quad (7)$$

A comparison of Equations 6 and 7 shows that the influence of soil can be taken into account by analysing a model of the form illustrated in Figure 8. This is possible by using an equivalent abutment height and by adding a horizontal (translational) spring at X. Equating all terms in $[K]$ and $[K_c]$ except the first, yields an equivalent abutment height of:

$$H_e = 3r^{-0.25} \quad (8)$$

To make the first terms equal requires a further adjustment which can be achieved by the addition of a spring at X of stiffness:

$$k = \frac{11EI_a r^{0.75}}{63} \quad (9)$$

In view of the approximate nature of Equation 5, this spring stiffness can be approximated to:

$$k = \frac{EI_a r^{0.75}}{6} \quad (10)$$

5 Example

An example serves to illustrate the simplified procedure. A 30m long 1.2m deep single-span reinforced concrete bridge is considered, supported by abutments extending to a depth of 6.5m below deck level. Young's modulus for the concrete was taken as 30×10^6 kPa and the coefficient of thermal expansion was taken as 12×10^{-6} per $^{\circ}\text{C}$. The effect of a uniform temperature increase of 21°C in the deck was investigated. Three different scenarios were considered with two different soil stiffnesses (E_s) and two thicknesses of abutment (t_a). Table 2 shows the various stiffnesses, and the equivalent heights and translational spring stiffnesses used for the simplified pinned based models of the form of Figure 8. Analysis of these frames was carried out using a plane frame program [19]. Figure 9 shows the simplified model for the first of these three frames.

| Frame No. | 1 | 2 | 3 |
|----------------------------|-----------|-----------|---------|
| E_s (kPa) | 400,000 | 40,000 | 40,000 |
| t_a (m) | 1.0 | 1.0 | 0.464 |
| EI_a (kNm ²) | 2,500,000 | 2,500,000 | 250,000 |
| $r = E_s/EI_a$ | 0.16 | 0.016 | 0.16 |
| H_e (m) | 4.74 | 8.44 | 4.74 |
| k (MN/m) | 105.4 | 18.7 | 10.5 |

Table 2: Parameters for Simplified Pinned Based Models

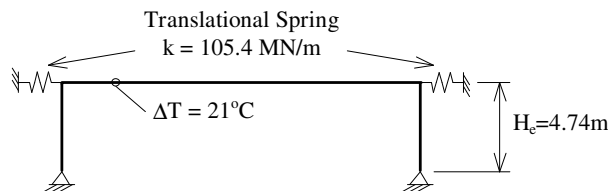


Figure 9: Simplified Plane Frame Model

The OASYS SAFE finite element computer program [17] was used to validate the results of the simplified analytical

method. An illustration of the mesh used and the predicted deformed shape of the bridge and the surrounding soil in response to a temperature increase in the deck is shown in Figure 10. Further analyses using this mesh indicated that, for the reasons discussed in Section 4, the inclusion of a strip footing at the base of the abutment and of soil at its inner face (as in Figure 10) had a negligible influence on predictions.

Table 3 compares the moments and axial forces predicted in the bridge deck by the SAFE analyses with that of the simplified approach. Both sets of predictions are seen to be in relatively good agreement; the main reason for the discrepancies being the approximate form of the matrix in Equation 5. More importantly, it is evident that the magnitudes of the induced forces are relatively small e.g. the maximum bending stress term, M/bd^2 , and the maximum axial stress of the three cases analysed are 0.13 N/mm^2 and 0.39 N/mm^2 respectively. Furthermore, it may be seen that the predictions are not overly sensitive to the choice of input parameters.

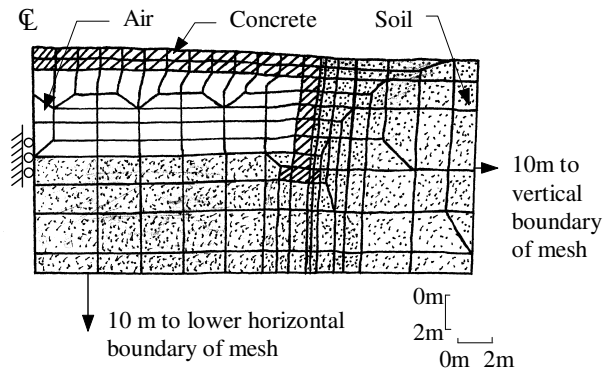


Figure 10: OASYS SAFE Deformed Mesh of Bridge and Surrounding Soil due to Temperature Increase in Deck

| Frame No. | 1 | 2 | 3 |
|----------------------------------|------|-----|-----|
| Simplified Plane Frame Method | | | |
| Moment (kNm) | -185 | -97 | -81 |
| Axial Force (kN) | 436 | 85 | 59 |
| OASYS SAFE Finite Element Method | | | |
| Moment (kNm) | -142 | -99 | -85 |
| Axial Force (kN) | 468 | 71 | 56 |

Table 3: Finite Element and Simplified Plane Frame Predictions of Bridge Deck Effects due to Temperature Increase of 21°C

6 Conclusions

A simple predictive model is developed for integral frame bridges subjected to the effects of thermal expansion. Only

bridges with high abutments are considered, where sliding resistance effects are not significant. The model uses an equivalent abutment height with a single translational spring to simulate the combined resistance offered by the actual abutment and the soil.

Expressions for the equivalent abutment height and the spring stiffness are derived using data obtained from parametric computer studies which modelled the backfill soil as a linear elastic continuum of stiffness E_s . Guidance on the selection of an appropriate value of E_s is deduced by application of research experience in the area of bridge abutments to a review and interpretation of recent high quality small strain stiffness measurements made in laboratory tests on cohesionless soils.

A typical example demonstrates the simplicity of application of the method using a frame analysis program such as is commonly used by bridge designers. The results are shown to comply well with those from a more elaborate Finite Element model of the soil and the structure.

References

1. The Highways Agency, The Scottish Office Industry Dept., The Welsh Office and the Dept. of the Environment for Northern Ireland, "Design for Durability" (Draft), BD 57/94, Vol.1, Section 3, Part 7, 1994.
2. O'Brien, E.J. and Flanagan, J.W., "Relief of creep/shrinkage stresses in integrally constructed bridges", in "Bridge Management 3, Inspection, Maintenance, Assessment and Repair", Harding, J.E., Parke, G.E.R. and Ryall, M.J. (Editors), E&FN Spon, London, 164-172, 1996.
3. Tatsuoka, F. and Shibuya, S., "Deformation characteristics of soils and rocks from field and laboratory tests" in "Proceedings of the 9th Asian Regional Conference on Soil Mechanics Foundation Engineering", Bangkok, Keynote Lecture, 53-114, 1991.
4. Jardine, R.J., "One perspective of the pre-failure deformation characteristics of some geomaterials", in "Proceedings of the International Symposium of Pre-failure Deformation Characteristics of Geomaterials", IS Hokkaido-Sapporo, 1, 855-886, 1994.
5. Lo Presti, D.C.F., "Measurement of shear deformation of geomaterials in the laboratory", in "Proceedings of the International Symposium of Pre-failure Deformation Characteristics of Geomaterials", IS Hokkaido-Sapporo, 1, 1067-1088, 1994.
6. Lehane, B.M., "Experimental investigation of pile behaviour using instrumented field piles", PhD Thesis, Imperial College (Univ. of London), 1992.
7. Paul, T.L., Lehane, B.M., Chapman, T.J. and Newman, R.L., "On the properties of a sandy gravel" in "Proceedings of the 13th International Conference on Soil Mechanics Foundation Engineering", New Delhi, 1, 29-32, 1994.
8. Johnson, J.G.A., Newman, R.L., Paul, T.S. and Pennington, D.S., "The measurement of strength, stiffness and in situ stress in the Thanet Beds using advanced techniques" in "Proceedings of ICE Conference on Recent Developments in Site Investigation Practice", London, (in press), 1995.
9. Park, C.S. and Tatsuoka, F., "Anisotropic strength and deformation of sands in plane strain compression", in "Proceedings of the 13th International Conference on Soil Mechanics Foundation Engineering", New Delhi, 1, 1-4, 1994.
10. Shibuya, S., Tatsuoka, F., Teachavorasinskun, S., Park, C-S and Abe, F., "Elastic properties of granular materials measured in the laboratory" in "Proceedings of the 10th European Conference on Soil Mechanics Foundation Engineering", Florence, 1, 163-166, 1991.
11. Tatsuoka, F., Kohata, Y., Mizumoto, K., Kim, Y-S., Ochi, K. and Shi, D., "Measuring small strain stiffness of soft rocks", in "Proceedings of the International Conference on Hard Soils and Soft Rocks", Athens, 1, 809-816, 1994.
12. Porovic, E. and Jardine, R.J., "Some observations on the static and dynamic shear stiffness of Ham River Sand", in "Proceedings of the International Symposium on Pre-failure Deformation Characteristics of Geomaterials", IS Hokkaido-Sapporo, 1, 25-30, 1994.
13. Tatsuoka, F. and Kohata, Y., "Stiffness of hard soils and soft rocks in engineering applications" in "Proceedings of the International Symposium on Pre-failure Deformation Characteristics of Geomaterials", IS Hokkaido-Sapporo, 2, 947-1065, 1994.
14. Springman, S.M. and Norrish, A.R.M., "Integral bridges - researchers' viewpoint", in "Seminar on the Design of Integral Bridges", Institution of Structural Engineers, London, jointly with IABSE and Highways Agency, 1-9, 23 Jan 1996, to be published.
15. Ingold, "The effects of compaction on retaining walls", *Geotechnique*, 29(3), 265-283, 1979.
16. Card, G.B. and Carder, D.R., "A literature review of the geotechnical aspects of the design of integral bridge abutments". UK Department of Transport, TRRL, Project Report 52, Transport Research Laboratory, Crowthorne, England, 1993.
17. OASYS, "User manuals for OASYS geotechnical programs", Ove Arup and Partners, 13 Fitzroy St., London W1P 6BQ, 1992.
18. Pappin, J.W., Simpson, B., Felton, P.J. and Raison, C., "Numerical analysis of flexible retaining walls", in "Proceedings of the International Conference on Numerical Methods in Engineering: Theory and Applications", Swansea, 1, 789-802, 1985.

19. STRAP, "User manual for STRAP structural analysis programs", ATIR Software, 13 Hahlait Saloniki Street, Tel-Aviv 69513, Israel, 1991.
20. Emerson, M., "Bridge temperatures estimated from shade temperature", UK Department of Transport, TRRL, Laboratory Report 696, Transport Research Laboratory, Crowthorne, England, 1976.